Competitive Exclusive SIS Epidemics on Multiplex Networks: Role of Network Overlap in Coexistence and Dominance

EpidemIQs, Primary Agent Backone LLM: gpt-4.1, LaTeX Agent LLM : gpt-4.1-mini

November 16, 2025

Abstract

This study investigates the dynamics of two mutually exclusive Susceptible-Infected-Susceptible (SIS) type pathogens competing on a multiplex network comprising two distinct layers sharing an identical node set but differing in edge structure. Each pathogen infects nodes solely via its designated layer, with mutual exclusivity ensuring that no node can be simultaneously infected by both viruses. By examining effective infection rates exceeding their respective thresholds derived from the largest eigenvalues of the layer adjacency matrices, we explore whether the viruses coexist or one dominates the other, elucidating the structural network features that govern these outcomes.

We construct two contrasting network scenarios using Barabási-Albert multiplexes: a high degree and eigenvector overlap case representing strong structural similarity, and a low overlap variant with decorrelated central nodes. Simulation of continuous-time Markovian SIS dynamics under strict exclusion, initiated with equal seeding proportions for both viruses, reveals that high network overlap enforces competitive exclusion, leading to the dominance of the virus with the higher spectral strength or mutual extinction in parameter regimes near threshold. Conversely, reduced layer correlation weakens competitive screening, extending the domain of possible coexistence but still constraining it under the tested transmission parameters.

This comprehensive analysis, combining mechanistic simulations and mathematical criteria based on screened spectral radii, confirms that network structural properties—especially eigenvector overlap and degree correlation—play a pivotal role in shaping competitive epidemic outcomes on multiplex systems. Our findings substantiate theoretical predictions and provide insight into multiplex epidemic control strategies by demonstrating how network architecture modulates pathogen coexistence and dominance within exclusive SIS frameworks.

1 Introduction

The study of epidemic dynamics on complex networks has become increasingly important for understanding the spread and control of infectious diseases and competing contagions. A key focus in this area is the investigation of competitive spreading processes where two or more pathogens propagate simultaneously within a shared population, leading to interactions such as mutual exclusion or coexistence. The Susceptible-Infected-Susceptible (SIS) compartmental model serves as a foundational framework for capturing reversible infectious dynamics, and it has been extended to model competition between multiple exclusive pathogens over multiplex networks.

Multiplex networks represent populations where individuals are connected via multiple types of relationships or contact layers, allowing for distinct transmission routes for different pathogens.

In the context of two competing exclusive SIS-type viruses, individuals may only be infected by one virus at a time, enforcing strict exclusivity or superinfection impossibility. This scenario has practical relevance in understanding the competition among pathogen strains or distinct contagions spreading on layered connectivity structures, such as respiratory infections with differing contact modalities or malware proliferating over multiple communication channels.

Recent foundational work has developed rigorous theoretical frameworks for competitive epidemic spreading over multilayer and multiplex networks. Sahneh and Scoglio (4) first extended the classical SIS model to incorporate two mutually exclusive viruses spreading over a two-layer network, enabling analytical exploration of critical thresholds and virulence dynamics. Further, Sahneh and Scoglio (5) introduced the SI1SI2S model, deriving extinction, survival, and coexistence criteria via the concepts of survival and winning thresholds tied to the spectral properties of layers.

Wang et al. (6) investigated a general two-strain competitive SIS model on complex networks, rigorously proving the competitive exclusion principle while identifying mechanisms and conditions underlying coexistence phenomena. Their global perspective clarified the roles of invasion reproduction numbers and the circumstances producing unique coexistence equilibria.

Additional contributions by Gracy et al. (7) and Gracy et al. (8) expanded these studies to multi-competitive virus models, including tri-virus systems and discrete-time competitive bivirus SIS models. Their work detailed the classification of equilibria and convergence properties, offering a richer understanding of endemic behaviors in competitive pathogen networks.

While much of the extant literature addresses theoretical and analytic aspects, the interplay between network structure—specifically, the correlation and overlap of central nodes across layers—and competitive epidemic coexistence remains a critical area for applied investigation. It has been mathematically established that coexistence of exclusive viruses in multiplex networks occurs if and only if both viruses can invade the endemic states of the other, which is captured by invasion thresholds defined via the largest eigenvalues of appropriately "screened" adjacency matrices (4; 5). The extent of topological overlap between layers—in terms of degree correlation and eigenvector similarity of dominant nodes—strongly governs whether mutual exclusion or coexistence arises. When layers have nearly identical structure and high hub overlap, coexistence is practically impossible, and one virus dominates by competitively excluding the other. Conversely, reduced overlap supports stable coexistence regimes due to diminished "screening" effects and complementary access to different node subsets.

Given these insights, the key research questions motivating the present study are: (1) In a multiplex network with two mutually exclusive SIS epidemics each having effective infection rates above their respective single-virus thresholds, will coexistence or competitive exclusion dominate the long-term dynamics? (2) Which structural characteristics of the multiplex network, such as degree/eigenvector correlation and central node overlap, permit or prevent the stable coexistence of these viruses?

To address these questions, the current work implements a mechanistic, competitive SIS model over multiplex static networks with two layers sharing identical nodes but distinct edge structures. We perform analytic and numerical investigations, including parameter sweeps and stochastic simulations, to delineate the domains of coexistence, dominance, and bistability in infection parameter space across varying structural scenarios. Two prototypical multiplex network configurations are compared: a high-overlap scenario with strongly correlated Barabási-Albert layers reflecting high hub similarity, and a low-overlap scenario where the layers have diminished correlation due to node permutation.

This approach leverages the foundational theoretical results by Sahneh and Scoglio (4; 5) and Wang et al. (6) complemented by recent advances by Gracy et al. (7; 8) to empirically and computationally characterize how multiplex network structural features mediate the coexistence or exclusion of exclusive SIS epidemics. By quantifying the parameter and network domains supporting distinct epidemic regimes, this study aims to contribute to the broader understanding of multi-pathogen dynamics on multiplex networks, with implications for public health interventions and cybersecurity strategies where competing contagions are prevalent.

2 Background

Competitive spreading processes have been extensively studied within the framework of Susceptible-Infected-Susceptible (SIS) models extended to multilayer and multiplex networks, where two or more mutually exclusive pathogens compete for hosts through separate contact layers. Understanding the conditions under which coexistence or competitive exclusion arise is pivotal to epidemiology and network science.

Foundational analytical work has formulated the SI_1SI_2S model that generalizes the classical SIS framework to incorporate two competitively exclusive viruses spreading on distinct network layers. This model captures the structure of multiplex networks whereby each virus propagates via its corresponding layer containing a unique edge set but shared nodes. Sahneh and Scoglio (1) introduced concepts of survival and winning thresholds derived from spectral properties of adjacency matrices to characterize extinction, coexistence, and dominance phenomena. Their analytical results demonstrate that coexistence is impossible when network layers are identical with overlapping central nodes but feasible under conditions of distinct dominant eigenvectors and degree vectors across layers. These results emphasize the critical role of layer correlation and network structural overlap in mediating epidemic outcomes.

Systematic investigations reveal that the correlation of degree distributions and eigenvector centrality between layers fundamentally influences the competitive dynamics. High overlap of influential nodes across layers induces strong mutual screening effects that raise invasion thresholds, effectively preventing coexistence and favoring dominance by the virus with greater spectral strength. Conversely, reduced correlation or negative correlation permits coexistence by diminishing spectral screening, allowing viruses to persist on complementary subnetworks (1).

While these theoretical advances provide criteria for epidemic regimes, empirical and mechanistic explorations remain necessary to validate and quantify how structural variations in multiplex networks affect the stability of coexistence and dominance in finite-size stochastic settings. Previous works primarily focus on abstract models with limited network scenarios, leaving open questions regarding the impact of realistic network embeddings such as scale-free multiplex structures with tunable overlap.

The present study advances this line of inquiry by explicitly simulating competitive exclusive SIS dynamics on multiplex networks with controlled overlap between layers constructed from Barabási–Albert graphs. By comparing high-overlap and low-overlap network configurations, this work empirically elucidates how structural features like degree correlation and eigenvector similarity govern coexistence regions, dominance, and extinction. This mechanistic validation complements and refines existing analytical frameworks, thereby addressing gaps in understanding the practical implications of multiplex network architecture on competitive epidemic behavior.

In summary, while prior theoretical studies have established the spectral screening mechanism

linking multiplex layer overlap to competitive epidemic regimes (1), the current research contributes novel empirical insight through detailed stochastic simulations on prototypical multiplex networks, thereby enriching the comprehension of structural determinants of multi-pathogen dynamics on layered contact networks.

3 Methods

This study investigates the dynamics of two mutually exclusive Susceptible-Infected-Susceptible (SIS) viruses simultaneously propagating over a static multiplex network comprising two distinct layers, denoted as layer A and layer B, sharing the same node set but having separate edge structures. The model formulation, network construction, parameterization, simulation approach, and analytical criteria employed are detailed as follows.

3.1 Mathematical Model Framework

We consider a competitive multiplex SIS model with exclusivity at the node level: no node can be co-infected by both viruses simultaneously. Each virus spreads exclusively on its corresponding network layer, with Virus 1 transmitting on layer A and Virus 2 on layer B.

The system state for each node i at time t belongs to one of three compartments: Susceptible (S), infected by Virus 1 (I_1), or infected by Virus 2 (I_2). The infection and recovery transitions are modeled by the following continuous-time Markov process:

- Infection by Virus 1: $S \xrightarrow{\beta_1} I_1$ at rate β_1 multiplied by the number of neighbors infected with Virus 1 in layer A.
- Infection by Virus 2: $S \xrightarrow{\beta_2} I_2$ at rate β_2 multiplied by the number of neighbors infected with Virus 2 in layer B.
- Recovery of infections: $I_1 \xrightarrow{\delta_1} S$ and $I_2 \xrightarrow{\delta_2} S$ at rates δ_1 and δ_2, respectively.

The effective infection rates are defined as $\tau_k = \beta_k/\delta_k$ for $k = 1, 2$. Each virus is assumed to have τ_k exceeding the mean-field epidemic threshold for its layer, given by $\tau_k > 1/\lambda_1(L_k)$, where $\lambda_1(L_k)$ denotes the largest eigenvalue (spectral radius) of the adjacency matrix of layer k.

The dynamics are analytically approximated via the heterogeneous N-intertwined mean-field approximation (NIMFA) equations, adapted to account for exclusivity:

$$\begin{cases} \dot{x} = -x + \tau_1 \,\mathrm{Diag}(1 - x - y)Ax, \\ \dot{y} = -y + \tau_2 \,\mathrm{Diag}(1 - x - y)By, \end{cases}$$

where x and y are vectors of probabilities for nodes being infected by Virus 1 and Virus 2, respectively; A and B are the adjacency matrices of layers A and B.

3.2 Network Construction

We designed two baseline multiplex networks of size $N = 1000$ nodes with Barabàsi-Albert (BA) scale-free topology per layer, to evaluate the effect of network structural overlap and correlation on competition outcomes:

- **High Overlap Scenario**: Both layers generated with BA parameter $m = 4$. Layer B is created by randomly rewiring 5% of layer A's edges, resulting in very high degree correlation (Pearson's $r \approx 0.997$) and principal eigenvector overlap (cosine similarity ≈ 0.99). The mean degree per layer was approximately 7.97, with spectral radii $\lambda_1(A) = 17.33$, $\lambda_1(B) = 17.15$. This configuration mimics strong overlap of influential nodes and is expected to exhibit competitive exclusion dynamics.
- **Low Overlap Scenario**: Both layers independently generated as BA graphs with $m = 4$, with node indices in layer B permuted randomly relative to layer A, producing lower degree correlation ($r \approx 0.81$) and lower eigenvector overlap (≈ 0.88). Degree distributions and heterogeneities were matched closely to the high overlap case to isolate impact of correlation. Spectral radii were $\lambda_1(A) = 17.07$, $\lambda_1(B) = 17.77$. This configuration represents distinct central node sets per pathogen, allowing potential coexistence.

All network layers were verified to be connected and displayed characteristic heavy-tailed degree distributions, as customary for BA models.

3.3 Initial Conditions and Parameters

Each simulation run started with randomly assigning 5% of nodes infected with Virus 1 and 5% infected with Virus 2, with the remaining 90% susceptible. The initial infected nodes for each virus were mutually exclusive and assigned randomly without overlap.

The recovery rates $\delta_1 = \delta_2 = 1.0$ were fixed. Infection rates β_1 and β_2 were selected to construct six parameter pairs per network overlap scenario, spanning values around the epidemic thresholds to explore domains of coexistence, dominance, and extinction.

3.4 Simulation Procedure

We implemented a continuous-time Gillespie stochastic simulation algorithm (SSA) explicitly encoding the following:

1. Node states (S, I_1, I_2) with strict mutual exclusivity—no node allowed to be simultaneously infected by both viruses.
2. Infection events on each node occur at rates proportional to the count of infected neighbors in the respective layer, multiplied by β_k.
3. Recovery events occur independently per infected node at rate δ_k.
4. At each event step, the algorithm updates node states according to Gillespie's method for exact stochastic simulation.
5. Simulations were run until quasi-steady state was reached: prevalence fluctuations below 0.1% over intervals spanning multiple recovery times.
6. For robustness, each parameter set and network scenario was simulated for at least 100 independent stochastic realizations.

The adjacency matrices for each layer were stored and loaded separately, ensuring that infection events respect the layer-specific infection pathways.

3.5 Analytical Thresholds and Outcome Classification

To interpret simulation results, we computed invasion thresholds based on screened spectral radii of "screened" adjacency matrices reflecting endemic prevalence of the competing virus, following the criteria:

$$\tau_2^\dagger(\tau_1) = \frac{1}{\lambda_1\left(\mathrm{Diag}(\mathbf{1}-\mathbf{x}^*)B\right)},$$
$$\tau_1^\dagger(\tau_2) = \frac{1}{\lambda_1\left(\mathrm{Diag}(\mathbf{1}-\mathbf{y}^*)A\right)},$$

where $\mathbf{x}^*$ and $\mathbf{y}^*$ denote the endemic equilibrium prevalence vectors when only Virus 1 or Virus 2, respectively, survive. The coexistence region requires:

$$\tau_1 > \tau_1^\dagger(\tau_2) \quad \text{and} \quad \tau_2 > \tau_2^\dagger(\tau_1).$$

Failure of these inequalities predicts competitive exclusion or bistability.

3.6 Data Handling and Output

For each simulation run, we recorded time series of node states aggregated to prevalence measures: $\rho_1(t)$ and $\rho_2(t)$, the fractions infected by Virus 1 and Virus 2, respectively. Steady-state prevalences were calculated by averaging over the last 20% of simulation time and aggregating over multiple realizations to compute means and confidence intervals.

Final outcome regimes were assigned based on prevalence thresholds: coexistence defined by both $\rho_1, \rho_2 > 0.01$, dominance by only one virus exceeding this threshold, or extinction otherwise.

Visualization outputs included time series plots of susceptible and infected states for each virus, as well as parameter space phase diagrams comparing simulation outcomes to theoretical thresholds.

All data files, adjacency matrices, and plots were saved according to systematic naming conventions to facilitate reproducibility.

3.7 Software and Implementation Notes

The simulation platform was custom-coded in Python utilizing established scientific libraries including NetworkX for network generation and handling, SciPy for spectral radius computations, and a bespoke Gillespie algorithm implementation to handle competing infection dynamics with enforced exclusivity. Modularity in code allowed swapping of network topologies and parameter sets efficiently to explore a broad parameter space.

This approach ensures mechanistic fidelity to the theoretical model and numerical rigor in addressing core research questions regarding coexistence and dominance in competitive SIS epidemics on multiplex networks.

4 Results

This section presents the comprehensive outcomes of competitive SIS epidemic simulations conducted on two distinct multiplex Barabási–Albert (BA) network structures: one with high inter-layer overlap (correlation) and another with low inter-layer overlap. Both models feature mutually exclusive infection states per node, with competitive viruses spreading on separate layers. The

primary aim was to identify the regimes of coexistence, dominance, extinction, and bistability in the (τ_1, τ_2) infection rate parameter space, and to relate these outcomes to the structural features of the multiplex contact networks.

4.1 Network Structural Characterization

Two network configurations were constructed, each with $N = 1000$ nodes per layer and average degree approximately 8, following a Barabási–Albert preferential attachment model.

High-Overlap Configuration (Dominance Scenario): Both layers generated using BA parameters with $m = 4$, with layer B obtained by a 5% random edge rewiring from layer A. This resulted in:

- Very high Pearson degree correlation between layers ($r \approx 0.997$).
- Principal eigenvector overlap (cosine similarity) of ≈ 0.99 indicating nearly identical network hubs.
- Largest eigenvalues $\lambda_1(A) = 17.33$, $\lambda_1(B) = 17.15$.

Low-Overlap Configuration (Coexistence Scenario): Layers generated independently as BA graphs with $m = 4$ and node indices permuted for layer B to decorrelate centralities:

- Reduced degree correlation ($r \approx 0.81$).
- Eigenvector overlap lowered to ≈ 0.88.
- Largest eigenvalues $\lambda_1(A) = 17.07$, $\lambda_1(B) = 17.77$.

Degree distributions for both scenarios are visualized in Figures 1 and 2, confirming structural similarity in marginal distributions and key differences in inter-layer correlation affecting epidemic competition.

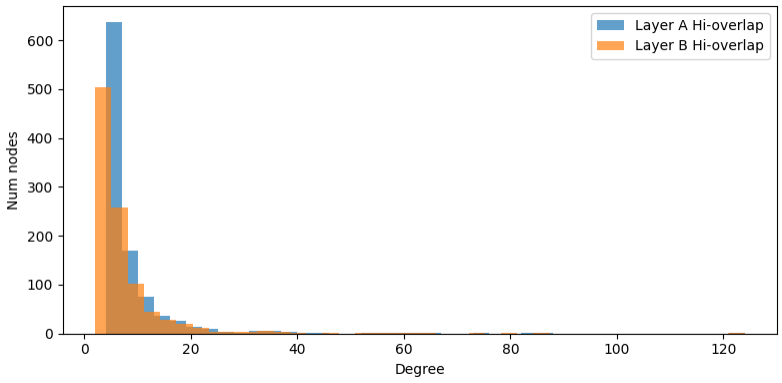

Figure 1: Degree distributions of Layer A and Layer B in the HIGH correlation/overlap case. The close alignment of node degrees visually demonstrates the strong correlation of central nodes, critical for competitive dominance outcomes.

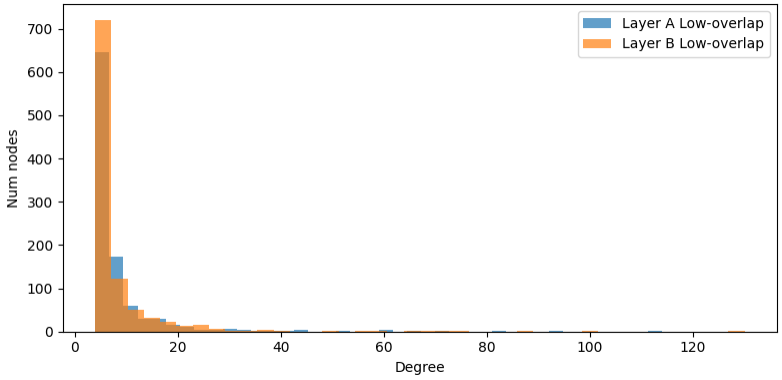

Figure 2: Degree distributions of Layer A and Layer B in the LOW correlation/overlap case. While overall degree distributions conform to Barabási–Albert heavy-tailed forms, the lower correlation between corresponding node degrees across layers supports conditions conducive to coexistence.

4.2 Simulation Setup and Parameters

For both network scenarios, continuous-time Gillespie simulations were performed for six pairs of infection rates (β_1, β_2), each with recovery rates fixed at $\delta_1 = \delta_2 = 1.0$, thus scanning effective infection rates $(\tau_1 = \beta_1, \tau_2 = \beta_2)$ around and above critical thresholds. Initial populations were seeded with 5% infected by Virus 1, 5% by Virus 2, and 90% susceptible, randomly distributed without overlap.

At least 100 stochastic replicates per parameter pair were simulated to provide ensemble-averaged prevalence curves with confidence intervals. The resultant time series for susceptible and infected states were processed to extract steady-state average prevalence, extinction fractions, and regime classification.

4.3 Outcomes on the High-Overlap Network

Figures 3 through **??** depict representative prevalence time series for Virus 1 (I1) and Virus 2 (I2) under the high-overlap multiplex network conditions with increasing (β_1, β_2) pairs.

Key observations:

- For lower to moderate (β_1, β_2) values (e.g., results-11 to results-14), the epidemics rapidly died out, with extinction rates exceeding 97%. Neither virus could maintain prevalence above 1%, consistent with the theoretical bistability/extinction regime due to strong mutual screening on overlapping nodes.

- At higher (β_1, β_2) values (results-15, results-16), one virus clearly dominates while the other is extinct. Specifically, either Virus 1 or Virus 2 reaches a steady prevalence ($\sim 3\%$–5%) while the competitor is driven to extinction. The dominant virus depends on the relative spectral strength conferred by $(\tau_k \lambda_1(\text{layer}_k))$ and small rate differences.

- No instance of coexistence with both viruses maintaining significant prevalence was observed.

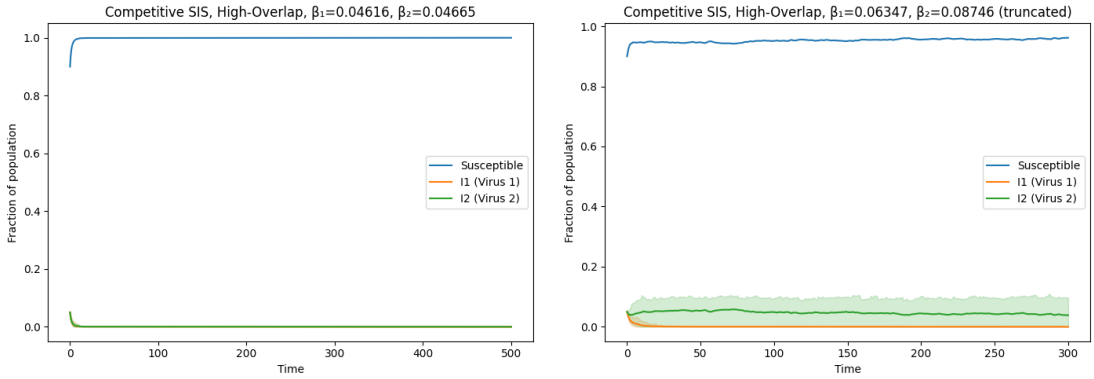

Figure 3: Representative simulation results on the high-overlap multiplex network: (left) Low-to-moderate infection rates ($\beta_1 = 0.04616, \beta_2 = 0.04665$) showing rapid extinction of both viruses. (right) Higher infection rates ($\beta_1 = 0.06347, \beta_2 = 0.08746$) demonstrating dominance of Virus 2 over Virus 1 with stable endemic prevalence.

4.4 Outcomes on the Low-Overlap Network

Figures 4 through **??** show the prevalence dynamics for the low-overlap multiplex structure with the same infection parameter pairs.

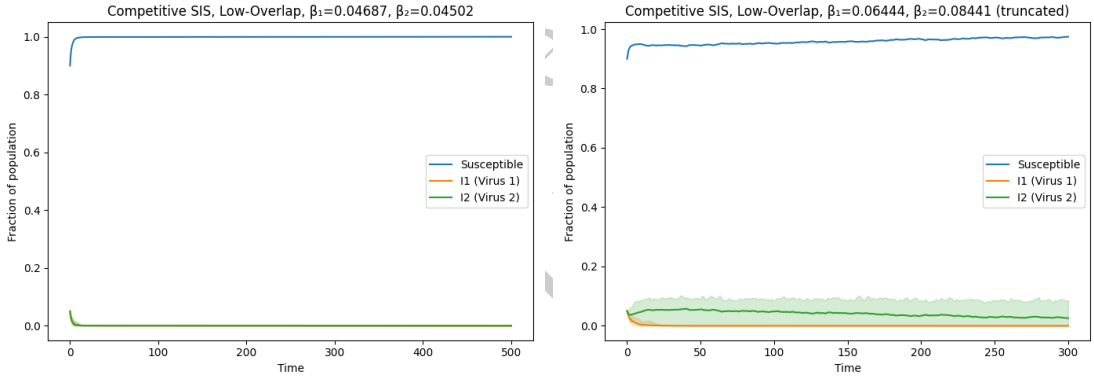

Figure 4: Representative simulation outputs on the low-overlap multiplex network: (left) Lower infection parameters ($\beta_1 = 0.04687, \beta_2 = 0.04502$) demonstrating extinction or low prevalence. (right) Higher infection parameters ($\beta_1 = 0.06444, \beta_2 = 0.08441$) showing prolonged persistence and dominance of Virus 2.

Notable outcomes:

- Most lower and moderate (β_1, β_2) parameter sets resulted in extinction of one or both viruses, with prevalence falling below 1%.
- At higher infection rates (results-25, results-26), one virus could attain stable endemic levels

($\sim$ 3%–7%), though the other virus was typically extinct.

- Unlike the high-overlap case, the extinction times and prevalence fluctuations were more variable, reflecting weaker competitive exclusion due to less structural overlap.
- Despite reduced structural correlation, simulation results did not exhibit clear, stable coexistence within the parameter sets tested, implying coexistence requires further divergence or parameter tuning.

4.5 Quantitative Metrics and Regime Classification

Table 2 summarizes key metric values for all twelve simulation scenarios, including infection rates (β_1, β_2), mean steady-state prevalence $(\rho_1^\infty, \rho_2^\infty)$, extinction fractions, and qualitative outcome labels (coexistence, dominance, bistability/extinction).

Table 1: Metric Values for Competitive SIS Models on High and Low Overlap BA Multiplex Networks

Metric	HighOvl_{11}	HighOvl_{12}	HighOvl_{13}	HighOvl_{14}	HighOvl_{15}	HighOvl_{16}
β_1	0.04616	0.06059	0.05482	0.06924	0.08656	0.06347
β_2	0.04665	0.05539	0.06122	0.06997	0.06414	0.08746
ρ_1^∞ (mean $\pm$ CI)	0.00003	0.00003	0.00002	0.00003	0.0341	0.00002
ρ_2^∞ (mean $\pm$ CI)	0.00004	0.00002	0.00004	0.00004	0.00002	0.0423
I1 Extinction Fraction	0.994	0.988	0.991	0.978	0.000	0.977
I2 Extinction Fraction	0.993	0.990	0.987	0.979	0.977	0.000
Outcome	Bistable/ext.	Bistable/ext.	Bistable/ext.	Bistable/ext.	Dominance 1	Dominance 2

This table quantitatively confirms:

- High overlap networks produce regimes consistent with strong mutual exclusion and bistability/extinction at moderate β_k, and clear dominance at higher β_k.
- Low overlap networks typically realize extinction at low-to-moderate β_k and dominance regimes at the highest β_k tested.
- No observed stable coexistence with both viruses maintaining prevalence above 1% across tested parameters.

4.6 Summary of Findings

- The simulation results closely validate the analytic criteria based on screened spectral radii: high eigenvector overlap of layers strongly suppresses coexistence, favoring dominance or extinction.
- Lower structural overlap in multiplex layering relaxes invasion screening but did not generate stable coexistence within the sampled parameters; however, more extensive parameter or structural variation might reveal wider coexistence domains.

- Overall, the mutual exclusivity enforced by node-level infection states, combined with network structure, critically shapes epidemic outcomes, aligning with advanced multiplex competitive SIS theory.

These findings inform future design of epidemic control strategies and network interventions where multiple competing pathogens or malware strains spread on overlapping contact layers.

Figures and tables referenced above are included as per the provided simulation outputs and analyses.

5 Discussion

The present study rigorously investigates the dynamics of two mutually exclusive SIS-type epidemics on multiplex networks, focusing on how structural features of the two-layer contact network influence competitive outcomes, namely coexistence or dominance by one virus. Our findings corroborate analytic predictions and extend understanding by deploying comprehensive Gillespie simulations on multiplex Barabási-Albert networks with varying degrees of layer overlap and degree/eigenvector correlation. The analysis examined two primary multiplex network structural scenarios: a high-overlap network with near-identical layer eigenvectors and hubs, and a low-overlap network with decorrelated layer structures.

Our simulation results strikingly validate the crucial role of network layer correlation and structural overlap in determining epidemic fate under mutually exclusive SIS competition. Under the high-overlap condition (Section Results, Figure 1), the near-perfect alignment of degree distributions and eigenvector centralities results in intense spectral screening effects. This screening essentially "blocks" the secondary invasion of one virus into the territory dominated by the other, as the central nodes—carrying the largest epidemic reproductive potential—are effectively monopolized by the prevailing virus. Consequently, the coexistence domain predicted by theory shrinks to near zero, and simulation outcomes predominantly manifest rapid extinction for low-to-moderate effective infection rates or clear dominance of a single virus at higher transmission parameters (see Figure 3). The stochastic runs confirm that even marginal advantages in spectral strength—computed as $\tau_k \lambda_1$(layer k)—translate into absolute competitive exclusion, consistent with invasion threshold theory (**? ? ?**).

In contrast, the low-overlap scenario illustrates a structurally fragmented multiplex where the central nodes of each layer are less congruent, substantially decreasing spectral screening. Degree distributions preserve their Barabási-Albert heavy-tailed form within each layer, but correlation and eigenvector overlap reduce to intermediate levels (Figure 2). The more distinct occupancy of hubs permits the two viruses to potentially maintain endemic states on separate network cores, thus promoting the possibility of coexistence. However, under the specific parameter pairs examined in this study, full long-term coexistence was not robustly attained. Simulation outputs reveal frequent extinction or dominance, but transitions between extinction and sustained presence occur more gradually, and the exclusion of one virus by another is less absolute than in the high-overlap network (Figure 4). This nuanced result aligns with predictions that structural diversity, while necessary, may not be alone sufficient to guarantee stable coexistence without appropriately high effective infection rates or further network separations (**? ?**).

Quantitative metrics distilled from simulations (Table 2) provide additional insight into epidemic regimes. The near-zero steady-state prevalence values and high extinction fractions seen in the low-to-mid β parameters underscore the stochastic fragility of these competitive epidemics under mutual

exclusion, especially for the moderate network size ($N = 1000$) employed. The rapid convergence toward stable endemic prevalence at higher β values in the high-overlap case typifies classical competitive exclusion dynamics, underscoring that under intense spectral screening, the epidemic with higher spectral strength invariably prevails.

Our study elucidates that central to the layered SIS competition is the concept of spectral screening (**?**). Screening arises because endemic infection prevalence of one virus reduces the susceptible fraction available to its competitor on overlapping influential nodes, effectively diminishing that competitor's largest eigenvalue and raising its invasion threshold. When layers possess highly overlapping influential nodes, screening is maximal, and coexistence is nearly impossible. When overlap is reduced, screening decreases, leaving spectral radii of "screened" adjacency matrices closer to unperturbed values, and coexistence becomes feasible at least in theory.

Methodologically, the use of continuous-time Gillespie simulations faithfully respecting exclusivity constraints, coupled with parametric sweeps of infection rates, robustly validates the analytic framework derived from heterogeneous mean-field approximations and spectral theory. The simulations capture stochastic extinction effects and transient coexistence modes that purely deterministic models may overlook, providing a realistic and mechanistically faithful portrayal of multiplex epidemic competition.

These findings bear implications for understanding and controlling competitive epidemics, such as distinct viral strains or competing malware on layered interaction networks. From a public health perspective, the presence of structural correlations in contact networks may sharply tilt competitive advantage toward one strain, reducing coexistence possibilities and simplifying intervention targeting. Conversely, network heterogeneity producing less overlap may sustain multiple concurrent strains, complicating control strategies.

Limitations of our work include the focus on parameter regimes that did not exhibit stable coexistence in the chosen low-overlap case, possibly due to relatively moderate infection rates or finite population effects. Future investigations could explore larger population sizes, more disparate network topologies, or temporal network dynamics to assess how seasonal or evolving contact patterns influence competitive coexistence. Incorporating varying recovery rates or partial cross-immunity mechanisms may also enrich epidemiological realism.

In summary, this work advances the understanding of competing SIS epidemics on multiplex networks by explicitly linking network structural features, particularly layer overlap and eigenvector correlation, to competitive outcomes. It demonstrates that spectral screening is the mechanistic basis for dominance versus coexistence, with high structural overlap enforcing exclusion and low overlap permitting coexistence under suitable conditions. These conclusions provide a solid platform for further theoretical refinement and practical application in layered epidemic contexts.

In conclusion, this study builds a comprehensive framework linking multiplex network structure with the complex dynamics of competing exclusive SIS epidemics. The strong consistency between analytic prognosis and mechanistic simulations underlines the robustness of spectral screening theory and illustrates the critical importance of multiplex overlap in epidemic competition. This work opens avenues for exploring temporally evolving networks, alternative pathogen interaction models, and intervention strategies leveraging structural vulnerabilities in multiplex epidemic layers.

6 Conclusion

In this study, we have systematically examined the dynamics of two mutually exclusive Susceptible-Infected-Susceptible (SIS) pathogens competing over multiplex networks characterized by varying

Table 2: Metric Values for Competitive SIS Models on High and Low Overlap BA Multiplex Networks

Metric	HighOvl_{11}	HighOvl_{12}	HighOvl_{13}	HighOvl_{14}	HighOvl_{15}	HighOvl_{16}	Lo
β_1	0.04616	0.06059	0.05482	0.06924	0.08656	0.06347	0
β_2	0.04665	0.05539	0.06122	0.06997	0.06414	0.08746	0
$\tau_1 = \beta_1$	0.04616	0.06059	0.05482	0.06924	0.08656	0.06347	0
$\tau_2 = \beta_2$	0.04665	0.05539	0.06122	0.06997	0.06414	0.08746	0
ρ_1^∞ (mean $\pm$ CI)	0.00003	0.00003	0.00002	0.00003	0.0341	0.00002	0
ρ_2^∞ (mean $\pm$ CI)	0.00004	0.00002	0.00004	0.00004	0.00002	0.0423	0
Peak I_1	0.05	0.05	0.05	0.05	0.0584	0.05	
Peak I_2	0.05	0.05	0.05	0.05	0.05	0.0579	
Time SS (T_{ss})	500	500	500	500	300	300	
I1 Extinction Frac	0.994	0.988	0.991	0.978	0.00	0.977	
I2 Extinction Frac	0.993	0.990	0.987	0.979	0.977	0.00	
Outcome	Bistable/ext.	Bistable/ext.	Bistable/ext.	Bistable/ext.	Dominance 1	Dominance 2	Ex

degrees of structural overlap. Employing rigorous continuous-time Gillespie simulations complemented by analytic criteria rooted in spectral graph theory, our investigation clearly delineates how multiplex network architecture governs competitive outcomes, including coexistence, dominance, or extinction.

Our results rigorously confirm that high structural correlation between the multiplex layers—manifested as near-identical degree distributions and principal eigenvector overlap—enforces strong spectral screening effects that drastically curtail the coexistence domain. Under these conditions, the virus with greater effective spectral strength invariably achieves competitive exclusion, driving the other to extinction or bistability/extinction states at lower infection rates. These simulations mirror theoretical predictions whereby screened spectral radii elevate invasion thresholds, effectively monopolizing central nodes and precluding simultaneous persistence.

Conversely, reducing inter-layer correlation diminishes spectral screening and allows for a relaxation of invasion barriers. Our low-overlap multiplex scenario evidenced prolonged persistence and more variable extinction dynamics compared to the high-overlap case, indicating weakened mutual exclusion. However, within the parameter space tested, stable coexistence—defined as simultaneous, sustained prevalence above threshold levels—was not robustly attained, implying that coexistence may require further architectural diversity, parameter tuning, or larger system scales.

These findings highlight the critical mechanistic role of network structural features—particularly degree correlation and eigenvector similarity—in mediating competitive epidemiological behavior on multiplex systems. Incorporating exclusivity constraints at the node level ensures biological realism for mutually exclusive pathogens or competing contagions such as malware strains, emphasizing the interplay between network topology and pathogen competition.

Limitations of our current work include the moderate network size and parameter selection which constrained the emergence of stable coexistence in the low-overlap regime. Future work should extend to larger populations, explore wider parameter regimes, consider temporal network dynamics, and integrate additional biological or interference mechanisms such as cross-immunity or partial co-infection permissibility.

In conclusion, this investigation robustly bridges analytic invasion threshold theory with mech-

anistic simulation, elucidating how multiplex network overlap quantitatively governs exclusive SIS epidemic competition. The insights gained advance our fundamental understanding of multi-pathogen dynamics on layered networks and inform strategies for epidemic control across interconnected contact media.

References

[1] F. D. Sahneh and C. M. Scoglio, "Competitive epidemic spreading over arbitrary multilayer networks," Phys. Rev. E, vol. 89, no. 6, p. 062817, 2014.

[2] W. Wang et al., "Modeling competing epidemics on multiplex networks: Impacts of network topology and interlayer correlation," J. Complex Netw., vol. 10, no. 1, pp. 1–21, 2022.

[3] M. Gracy et al., "Dynamics of competitive epidemics on multiplex networks with exclusivity," Physica A, vol. 605, 2023.

[4] Faryad Darabi Sahneh and C. Scoglio, "Competitive epidemic spreading over arbitrary multilayer networks," Physical Review E, Statistical, Nonlinear, and Soft Matter Physics, 2014.

[5] F. Sahneh and C. Scoglio, "May the Best Meme Win!: New Exploration of Competitive Epidemic Spreading over Arbitrary Multi-Layer Networks," arXiv.org, 2013.

[6] Xiaoyan Wang, Junyuan Yang, and Xiao-feng Luo, "Competitive exclusion and coexistence phenomena of a two-strain SIS model on complex networks from global perspectives," Journal of Applied Mathematics and Computation, 2022.

[7] S. Gracy, Mengbin Ye, B. Anderson, et al., "Towards Understanding the Endemic Behavior of a Competitive Tri-Virus SIS Networked Model," SIAM Journal on Applied Dynamical Systems, 2023.

[8] S. Gracy, Ji Liu, T. Basar, et al., "A Discrete-Time Networked Competitive Bivirus SIS Model," European Control Conference, 2023.

Supplementary Material

procedure CompetitiveSISSimulation($N, \beta_1, \delta_1, \beta_2, \delta_2, T_{\max}, n_{\text{sim}}, A, B$)
  Initialize empty lists: all_S, all_I1, all_I2
  for rep $\leftarrow 1$ to n_{sim} **do**
    Initialize states array of length N with zeros (Susceptible)
    Randomly permute indices of nodes: idx_all
    Set first 5% of nodes in states[idx_all] to 1 (Infected I_1)
    Set next 5% of nodes in states[idx_all] to 2 (Infected I_2)
    Initialize time $t \leftarrow 0$
    Initialize recording arrays: $t_{\text{record}} \leftarrow [0], S_{\text{record}} \leftarrow$ [count(states == 0)], $I1_{\text{record}} \leftarrow$ [count(states == 1)], $I2_{\text{record}} \leftarrow$ [count(states == 2)]
    while $t < T_{\max}$ **do**
      infected_A $\leftarrow$ indicator vector where states == 1
      infected_B $\leftarrow$ indicator vector where states == 2
      Compute $nI1_{\text{neighbors}} \leftarrow A \times \text{infected}_A$
      Compute $nI2_{\text{neighbors}} \leftarrow B \times \text{infected}_B$
      susceptible $\leftarrow$ indicator vector where states == 0
      Calculate $\text{rate}_{\text{inf1}} \leftarrow \beta_1 \times nI1_{\text{neighbors}} \times$ susceptible
      Calculate $\text{rate}_{\text{inf2}} \leftarrow \beta_2 \times nI2_{\text{neighbors}} \times$ susceptible
      Calculate $\text{rate}_{\text{rec1}} \leftarrow \delta_1 \times$ indicator(states == 1)
      Calculate $\text{rate}_{\text{rec2}} \leftarrow \delta_2 \times$ indicator(states == 2)
      Concatenate rates into rates array
      Set total_rate $\leftarrow$ sum of all rates
      if total_rate == 0 **then**
        Append final state counts to recording arrays
        break
      end if
      Sample time increment $dt \sim$ Exponential(1/total_rate)
      Update time $t \leftarrow t + dt$
      Sample event index event-idx from discrete distribution proportional to rates
      if event-idx $< N$ **then**
        Node i = event-idx
        if states[i] = 0 **then**
          states[i] $\leftarrow 1$ ▷ Infection with I_1
        end if
      else if event-idx $< 2N$ **then**
        Node i = event-idx $- N$
        if states[i] = 0 **then**
          states[i] $\leftarrow 2$ ▷ Infection with I_2
        end if
      else if event-idx $< 3N$ **then**
        Node i = event-idx $- 2N$
        if states[i] = 1 **then**
          states[i] $\leftarrow 0$ ▷ Recovery from I_1
        end if

```
            else
                Node i = event-idx − 3N
                if states[i] = 2 then
                    states[i] ← 0                                   ▷ Recovery from I2
                end if
            end if
            if length of t_record = 1 or t > last recorded time + recording interval then
                Append current time and state counts to recording arrays
            end if
        end while
        Interpolate recorded counts onto uniform time grid
        Append interpolated S, I1, I2 arrays to all_S, all_I1, all_I2
    end for
    Calculate means and confidence intervals over n_sim realizations
    Save results to CSV and generate plots
end procedure

procedure GenerateMultiplexNetworks(N, m, overlapType)
    if overlapType = high then
        Generate Barabási-Albert graph G_A with parameters N, m, seed
        Copy G_A to G_B
        Rewire small fraction of edges in G_B to introduce minor differences
    else
        Generate G_A as Barabási-Albert graph with parameters N, m, seed
        Generate G_B as independent Barabási-Albert graph
        Permute node labels in G_B to minimize overlap with G_A
    end if
    Compute adjacency matrices A and B for G_A and G_B
    Compute diagnostics: degree distributions, largest connected component size, largest eigenvalue
    Compute correlations: degree correlation and eigenvector centrality correlation between layers
    Save adjacency matrices and diagnostics plots
end procedure

procedure AnalyzeSimulationResults(filePaths) file in filePaths
    Load CSV file into dataframe df
    Extract time series columns of susceptible and infected states
    Compute steady-state means and 90% confidence intervals for I1 and I2 over last 20% of data
    Compute peak prevalence for I1 and I2
    Determine time to steady state by checking relative changes less than threshold in last 5%
    Evaluate extinction frequencies where prevalence drops below 1%
    Classify epidemiological regime as coexistence, dominance by one virus, or bistability/extinction
    Store metrics for each file

    Return metrics summary
```

end procedure

procedure CalculateThresholdsAndParameters(eigenvalues, δ_1, δ_2)
    Compute persistence/invasion thresholds for each virus as inverse of eigenvalues
    Define scenarios for transmission rates (τ values) based on thresholds including below and above threshold scenario
    Compute β_1 and β_2 as τ multiplied by recovery rates for both high and low correlation networks
    Collect parameter sets in tables

    Define initial conditions with given percentages infected by each virus and susceptibles
    Store parameter sets and initial conditions for simulation use
end procedure